

Study of terahertz spoof surface plasmons on subwavelength gratings with dielectric substance in grooves

V.V. Bulgakova^{a,b}, V.V. Gerasimov^a, A.G. Lemzyakov^a, B.G. Goldenberg^a

^a Budker Institute of Nuclear Physics, 630090, Lavrentieva prospect, 11, Novosibirsk, Russia

^b Novosibirsk State Technical University, 630073, Karl Marx Street, 20, Novosibirsk, Russia

Abstract

Terahertz (THz) plasmonic devices based on periodical corrugated structures are promising for sensing applications in biology and medicine but have not been developed so far because spoof surface plasmons (SSPs) on such structures were studied insufficiently in the THz spectral range. In the paper, the propagation of THz SSPs along one-dimensional subwavelength rectangular plane gratings with a dielectric substance in the grooves was studied and optimal parameters of gratings (period, aspect ratio and groove depth) for sensing of dielectric were found. First grating samples were made and tested using the THz radiation of the Novosibirsk free electron laser.

Keywords: spoof surface plasmons; subwavelength gratings; terahertz region; bio-medical sensing

1. Introduction

Surface plasmons (SPs) are electromagnetic excitations propagating at an interface between a conductor and a dielectric, evanescently confined in the perpendicular direction. These electromagnetic surface waves arise via the coupling of the electromagnetic fields to oscillations of the conductor electron plasma [1].

Surface plasmons have been studied well in the visible and infrared ranges but insufficiently in the terahertz (THz) region because no appropriate THz sources and detectors have been developed until recently [2]. The terahertz spectral range is located between the microwave and far-infrared regions and covers wavelengths from 30 to 300 μm . This radiation is of great importance for biological, medical and security sensing applications as it is nonionizing and many rotational and vibrational modes of complex intra- and extra-molecule bonds of biological substances lie in the THz frequency range [3]. Today researchers have a growing interest to metamaterials, i.e. periodical subwavelength structures with special optical properties that enable manipulating electromagnetic waves. Surface waves propagating along a metamaterial structure (named in literature “spoof surface plasmons” (SSPs)) are bound electromagnetic surface modes having a high field coupling with the structure even in the case of perfect electrical conductor (PEC) material [4]. As metals in the THz range are like PECs, SSPs are very promising for the THz plasmonics, especially for sensing applications. High confinement of SSPs allows enhancing the light–matter interaction, as well as using small sample volumes.

In this paper, the possibility of developing a THz plasmon sensor based on a one-dimensional rectangular grating was studied. A theoretical analysis of the length of SSP propagation along the grating has been performed, and optimal grating parameters (period, aspect ratio and groove depth) for sensing of polar and non-polar liquids were found. Numerical simulations in CST Microwaves studio of electromagnetic field near the grating structure have been done to verify localization of the field of surface plasmon in the grooves. A set of gratings on plane glass samples with gold covering was made and tested using the terahertz radiation of the Novosibirsk free electron laser.

2. Theoretical analysis of grating structure

2.1. Brief theory

Spoof surface plasmons (SSPs) are slowing surface modes propagating along an insulator–corrugated metal structure boundary. A periodical structure can play a role of an artificial dielectric layer with reactive impedance. The surface current in the structure is higher than that on a plane surface due to a larger current path in the grooves. The phase velocity of SSPs is small at certain sizes of the structure with respect to the radiation wavelength λ .

Let us consider a one-dimensional periodical rectangular structure with a period d , groove width a , and groove depth h (see Fig. 1). The wave-vector of SSPs propagating along the grooves is defined by the dispersion relation [5] as follows:

$$k_p = \left[\varepsilon_d k_0^2 + \left(\frac{a \varepsilon_d}{d \varepsilon_g} \right)^2 k_g^2 \operatorname{tg}^2(k_g h) \right]^{1/2}, \quad (1)$$

where $k_0 = 2\pi / \lambda$ is the wave-vector of free wave in vacuum; ε_d is the dielectric permittivity of the external medium; ε_g is the permittivity of the substance in the grooves; k_g is the wave-vector of the wave propagating in the grooves. k_g can be expressed as

$$k_g = k_0 \sqrt{\epsilon_g} \left(1 + \frac{l_s(i+1)}{a}\right)^{1/2}. \quad (2)$$

Eq. (1) takes into account the finite conductivity of the metal ϵ_m via the skin depth $l_s = (k_0 \operatorname{Re} \sqrt{-\epsilon_m})^{-1}$ ($l_s \approx 30\text{--}120$ nm in the THz range [6]).

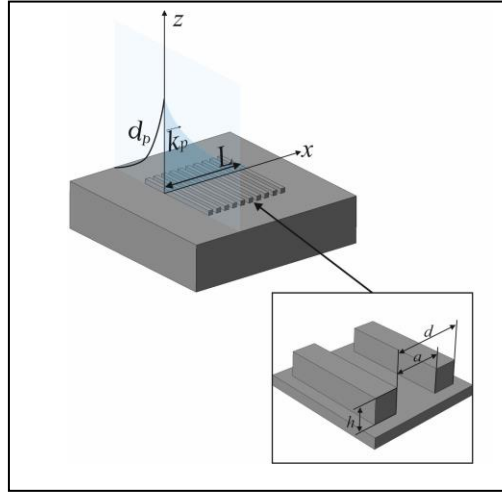


Fig. 1. Scheme of one-dimensional periodical rectangular structure.

2.2. Analytical calculations

The length $L = 1/2 \operatorname{Im}(k_p)$ of SSP propagation along the guiding structure with parameters $d = 110 \mu\text{m}$ and $a = 55 \mu\text{m}$ was calculated using Eq. (1) as a function of the groove depth h (Fig. 2) for the case of gold surface with a dielectric permittivity $\epsilon_m = -103360 + i \cdot 301810$ in the THz range and liquid water inside the grooves with $\epsilon_g = 3.79 + i \cdot 1.8$. Calculations were done for a radiation wavelength $\lambda = 130 \mu\text{m}$.

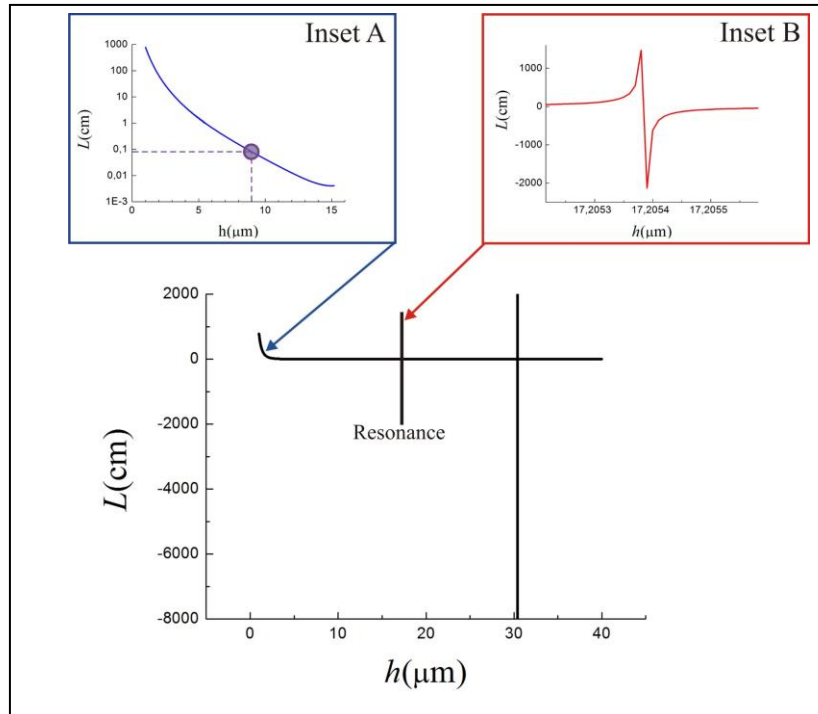
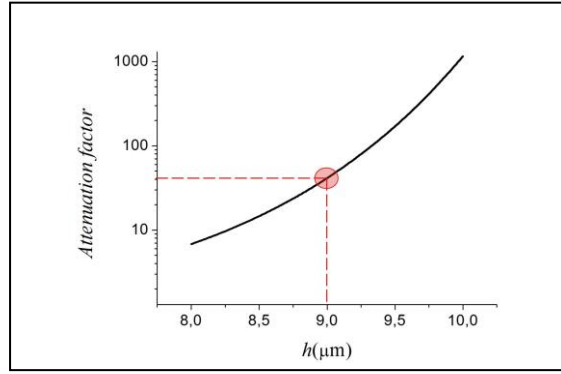


Fig. 2. Length of propagation of SSPs vs. the groove depth, calculated using Eq. (1) for one-dimensional gold grating with water in grooves. Groove period: $d = 110 \mu\text{m}$; groove width: $a = 55 \mu\text{m}$; radiation wavelength: $\lambda = 130 \mu\text{m}$.

The vertical lines in the $L(h)$ dependence correspond to resonances (see the detailed graph in the inset B, Fig. 2) arising when the argument of the tangent function $k_g h \rightarrow \pi/2$. As metals have high conductivity in the THz range, $k_g \approx k_0$ and the resonance



occurs when $h \approx \lambda_0 / 4\sqrt{\epsilon_g}$. The negative value of L in a region with a resonance means that the corrugated structure becomes a metamaterial with a negative refractive index. At a resonance, a groove plays the role of a quarter-wavelength antenna, which reradiates the SSPs into bulk waves. As losses of SSPs on the grating are large in the case of resonance, we chose a region far from the resonance (see inset A in Fig. 2). On the one hand, for high sensitivity of plasmon sensor we need to take deeper grooves (higher h), which correspond to the shortest L , and on the other hand, L must be large enough to be measurable with our experimental technique (see Sec. 4).

Fig. 3. Attenuation of SSPs after filling of grating grooves with water drop (diameter $w \approx 3$ mm).

If we put a water drop with a diameter $w \approx 3$ mm on the grating, the signal of SSPs will drop with a factor

$$A = \exp((\alpha_s - \alpha_0)w), \quad (3)$$

were $\alpha_s = 2\text{Im}(k_s^{\text{water}})$ is the absorption coefficient of the SSPs propagating along the grating filled with liquid water, and $\alpha_0 = 2\text{Im}(k_s^{\text{air}})$ is that with the grating grooves filled with air. The dependence of the attenuation factor on the groove depth h calculated using (3) is shown in Fig. 3. For instance, with $h \approx 9 \mu\text{m}$ the SSP signal falls about 40-fold, which meets our requirements for plasmonic sensing. The optimal groove depth was found for ethanol in the same way. The resulting grating parameters are shown in Table 1.

Table 1. Optimal parameters of one-dimensional gratings found for water and ethanol sensing

Grating parameter	Water	Ethanol
Period d (μm)	110	110
Groove width a (μm)	55	55
Groove depth h (μm)	9	19

For instance, if the plasmon signal drops 40-fold after propagation of SSPs along a 20-mm grating structure, the propagation length L must be about 1–10 cm, which corresponds to $h \approx 9 \mu\text{m}$ (inset A, Fig. 2). Choosing of the groove depth also depends on the wetting properties: shallow gratings with a small h are better wetted with liquids (see Sec. 3.2).

2.3. Numerical simulations

We calculated the electromagnetic field (EMF) of SSPs propagating along a one-dimensional grating (see Fig. 1) using CST Microwave studio. An example of EMF density distribution for a grating with $d = 110 \mu\text{m}$, $a = 55 \mu\text{m}$, $h = 9 \mu\text{m}$, and $\lambda = 130 \mu\text{m}$ is shown in Fig. 4. It can be seen that the EMF is confined near the grating and localized in the grooves, which is very important for plasmonic biosensor applications.

3. Experimental samples

We made experimental samples with one-dimensional rectangular gratings. The grating parameters (period, aspect ratio and groove depth) were chosen based on results of theoretical analyses (see Sec. 2.2). The gratings were deposited on glass substrates using UV and multibeam X-ray lithography techniques (details see below).

3.1. Sample preparation

Gratings (20x20 mm) with a period $d = 110 \mu\text{m}$ and aspect ratio of 1:1 were deposited on the optically polished upper faces of 40x40x3mm³ glass substrates using UV lithography. The polished surfaces were covered with a thin layer of the photoresist

SU-8 using the spin-coating technique. The thickness of the layer was set through variation of the rotational speed of the centrifuge. The resist was irradiated by an UV light ($\lambda=365$ nm) through a photomask. Then the resist was subjected to a plasma discharge in the oxygen atmosphere and covered with a gold film $0.3\text{ }\mu\text{m}$ thick using DC magnetron sputtering. A grating photo recorded with scanning electron microscopy (SEM) is shown in Fig. 1 (a).

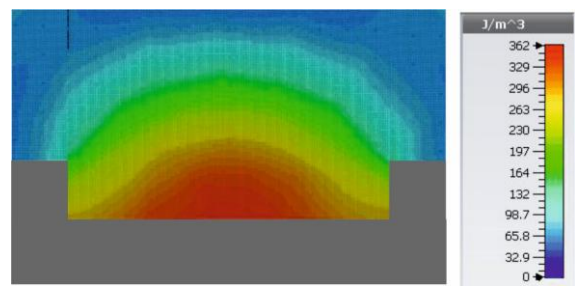


Fig. 4. Simulations of electromagnetic field density distribution of SSPs around one-dimensional grating ($d = 110\text{ }\mu\text{m}$, $a = 55\text{ }\mu\text{m}$, $h = 9\text{ }\mu\text{m}$) with air in grooves.

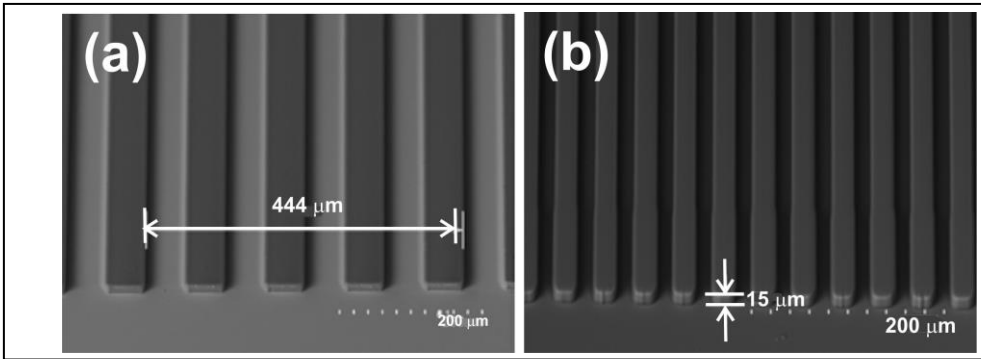


Fig. 5. SEM photo of grating with period $d = 111\text{ }\mu\text{m}$ (a) and $d = 40\text{ }\mu\text{m}$ (b), made using UV lithography.

Besides that, we made gratings with a smaller period $d \approx 40\text{ }\mu\text{m}$ and aspect ratio of 1:1. According to the theory, these gratings must produce less diffractive radiative losses (as $d<\lambda/2$ [7]) and, consequently, larger SSP propagation length. With such samples we used multibeam X-ray lithography as more preferable for rectangular periodical structures with a small period and deep groove [8]. The resist SU-8 was exposed to synchrotron radiation through an X-ray pattern at the station LIGA of Budker INP SB RAS. The deviation of the geometrical sizes of sample structures (Fig. 1 (b)) along the grating was less than $1\text{ }\mu\text{m}$.

3.2. Wettability testing

The experimental results and some theoretical papers demonstrated that a clean plane gold surface is hydrophilic [9]. The angle of contact with water θ_c was less than 65° , θ_c is expected to decrease in the case of corrugation of the surface. We tested our samples for water wettability. To this end, a water drop (volume $\approx 0.002\text{ ml}$) was put on the sample surface. The drop diameter D and height H were measured and the contact angle was calculated using well known expression

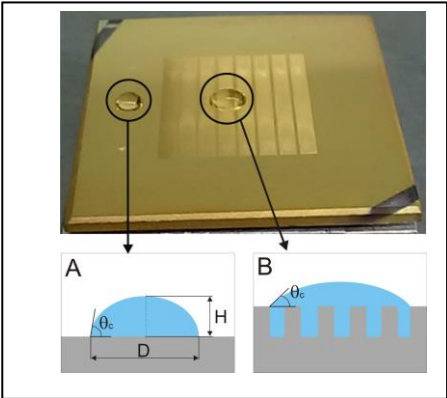


Fig. 6. Example of figure caption.

$$\theta_c = \arccos \left[\frac{(D/2)^2 - H^2}{(D/2)^2 + H^2} \right] \tag{3}$$

Results for several samples are shown in Table 1. With a smooth gold surface, the contact angle $\theta_c \approx 74^\circ$, which is in accord with literature data [10]. The gratings with the small period ($d = 40 \mu\text{m}$) are hydrophobic, and the gratings with the long period ($d \approx 112 \mu\text{m}$) are hydrophilic. Besides, the less was the groove depth, the better was the wettability. With a grating with $h = 9 \mu\text{m}$ the contact angle was less than with a smooth gold surface. Because better wettability of grating is required for higher sensitivity of plasmon sensor, we should use shallow gratings with a large period.

Table 2. Contact angle of wetting

Sample	Contact angle θ_c (deg)
Smooth gold surface	74
Grating № 3 ($d = 112 \mu\text{m}$; $a = 57 \mu\text{m}$; $h = 17 \mu\text{m}$)	74
Grating № 7 ($d = 113 \mu\text{m}$; $a = 58.2 \mu\text{m}$; $h = 9 \mu\text{m}$)	68
Grating № 8 ($a = 15 \mu\text{m}$; $d = 40 \mu\text{m}$; $h = 19 \mu\text{m}$)	95

4. Experiments in the THz range

A gold mirror was directing the monochromatic linearly polarized THz radiation ($\lambda = 130 \mu\text{m}$) generated by the Novosibirsk free electron laser [11] (see Fig. 3) on a coupling grating at an incident angle ϕ . A ruled grating was fabricated by milling of a given periodic profile on a monolithic aluminum substrate [12]. The grating had a sawtooth profile with a period $\Lambda=0.3 \text{ mm}$ and the groove height $h=0.1 \text{ mm}$, see inset A in Fig. 3. The coupling angle was $\phi \approx 37^\circ$, which corresponds to the theoretically predicted one. The launched SSPs were passed along the sample grating (see inset B in Fig. 3), uncoupled into a bulk wave at the edge of a 45° cylinder (curvature radius $R=60 \text{ mm}$) and detected using an opto-acoustic Goley cell (TYDEX). The upper faces of the coupling grating and decoupling cylinder were covered with a gold layer $1 \mu\text{m}$ thick. For reducing of the SSP radiative losses on the cylindrical surface, it was optionally covered with a $0.5\text{-}\mu\text{m}$ ZnS dielectric layer. We used the cylindrical geometry to screen the detector from parasitic bulk waves produced on the surface imperfections and junctions between the SSP guiding elements. For the same reason, the half part of the input aperture of the detector was screened with a metal diaphragm. The input THz beam was modulated with a chopping frequency 15 Hz and controlled with a pyroelectric detector.

We tested the transmission of SSPs through the sample gratings through measurement of the SSP signal at the edge of the uncoupling cylinder. We found that (1) the transmission was maximal with the shortest-period grating ($d \approx 40 \mu\text{m}$ and $h = 19 \mu\text{m}$) and (2) the less was the groove depth, the higher was the SSP transmission,. These results are in accord with the theory ([6] and see Sec. 2.2).

Then we tested the attenuation of the SSP signal after putting ethanol or liquid water drops (volume $\approx 0.002 \text{ ml}$) on smooth and grating surfaces (see Fig. 4). The following was revealed: the less was the groove depth, the higher was the SSP attenuation. It means that liquids on surfaces with deep grooves are less sensed with spoof plasmon electromagnetic field due to the less wettability of the surface (see Sec. 3.2). To increase the sensitivity of plasmon sensor we need to use shallow gratings with high wettability.

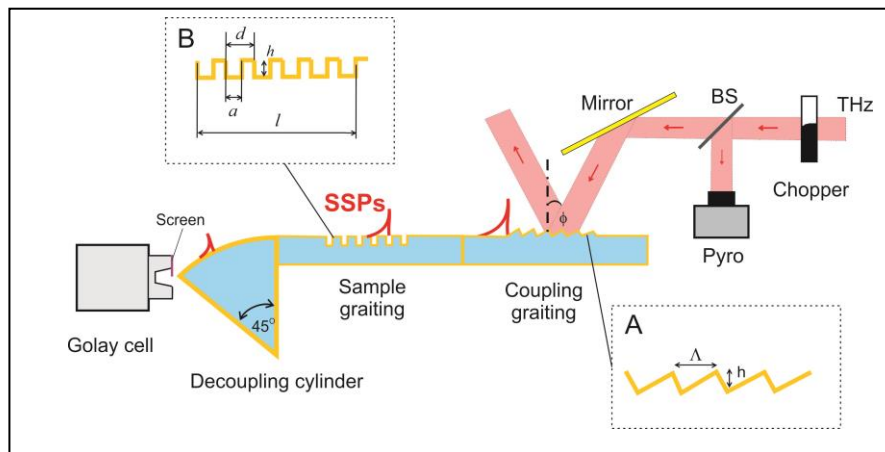


Fig. 7. Experimental scheme of SSP transmission through sample grating. Grating structures are shown in insets: A (coupling grating) and B (sample grating).

5. Conclusion

The characteristics of THz spoof surface plasmons propagating along a one-dimensional rectangular subwavelength plane grating with a dielectric substance in the grooves have been analyzed. Numerical calculations of the plasmon electromagnetic field demonstrated that it was localized inside the grooves and could strongly interact with the substance under study. Optimal parameters of gratings (period, aspect ratio and groove depth) for sensing of polar and non-polar liquids were found at a wavelength of $130 \mu\text{m}$. The first grating samples were made using UV and multibeam X ray lithography techniques. Testing of

the water and ethanol wettability of the samples and first experiments using THz radiation ($\lambda = 130 \mu\text{m}$) of the Novosibirsk free electron laser showed that shallow gratings were more preferable for plasmon sensing applications.

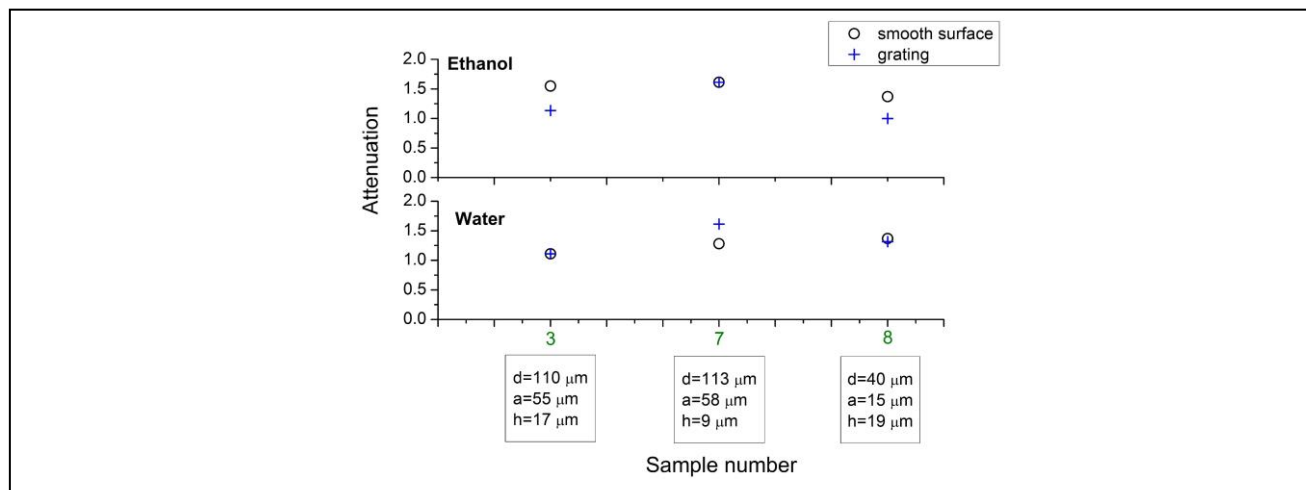


Fig. 8. SSP attenuation with ethanol or water drops put on smooth gold surfaces (circles) and gratings (crosses). The number of samples with the corresponding grating parameters is depicted along the x-axis.

Acknowledgements

The investigations were supported by the Russian Science Foundation (grant No. 14-50-00080) and Russian Foundation for Basic Research (grant No. 16-32-00678). The Siberian Synchrotron and Terahertz Radiation Center equipment and free electron laser were employed in the experiments.

References

- [1] Maier, S.A. Plasmonics: Fundamentals and Applications. Springer, 2007. - 224 p.[2] X. Yin et al., Terahertz Imaging for Biomedical Applications: Pattern Recognition and Tomographic Reconstruction / Springer Science+Business Media, LLC, 2012 – P. 9-26.
- [2] Yin, X. et al. Terahertz Imaging for Biomedical Applications: Pattern Recognition and Tomographic Reconstruction / Springer Science+Business Media, LLC, 2012 – P. 9-26.
- [3] Siegel, P.H. Terahertz Technology in Biology and Medicine // IEEE Transactions on microwave theory and techniques. – 2004. - Vol. 52(10). – P. 2438-2447.
- [4] Pendry, J.B.Martin-Moreno, L.; Garcia-Vidal, F.J. Mimicking surface plasmons with structured surfaces // Science. - 2004. - Vol. 305 (5685). P. 847-848.
- [5] Rusina, A., Durach, M., Stockman, M.I. Theory of spoof plasmons in real metals // Applied Physics A, June 2010.
- [6] Князев, Б.А., Кузьмин, А.В. Поверхностные электромагнитные волны: от видимого диапазона до микроволн // Вестник НГУ. Серия: Физика. – 2007. Том 2 (1). – С. 108-122.
- [7] Popov, E., Tsonev, L. Losses of plasmon surface waves on metallic grating // Journal of modern optics. - 1990. - Vol. 37 (3). - P. 379-387.
- [8] Goldenberg, B.G., Lemzyakov, A.G., Nazmov, V.P., Pindyurin, V.F., Zelinsky, A.G. Multibeam X-ray lithography to form deep regular microstructures // Journal of Surface Investigation: X-Ray, Synchrotron and Neutron Techniques. - 2016. Vol. 10(1). – P. 92-95.
- [9] Smith, T. The hydrophilic nature of a clean gold surface // Journal of Colloid and Interface Science, Vol. 75, No. 1, May 1980.
- [10] van Zwol, P. J., Palasantzas, G., De Hosson, J.Th.M. Influence of roughness on capillary forces between hydrophilic surfaces // Phys. Rev. E. – 2016. Vol. 78. – P. 031606.
- [11] Shevchenko, O.A. et al. The Novosibirsk Free Electron Laser – Unique Source of Terahertz and Infrared Coherent Radiation // Physics Procedia. – 2016. Vol. 84. – P. 13–18.
- [12] Nazarov, M.M., Mukina, L.S., Shuvaev, A.V., Sapozhnikov, D.A., Shkurinov, A.P., Trofimov, V.A. Excitation and propagation of surface electromagnetic waves studied by terahertz spectroscopy // Laser Physics Letters. – 2005. Vol. 2 (10). –P. 471-475.